Allergy, Asthma &
Immunology Research

AAIR

Original Article

Check for updates

OASL1-Mediated Inhibition of Type I IFN Reduces Influenza A Infection-Induced Airway Inflammation by Regulating ILC2s

Yuna Chang [ID],[1,2] Ji-Seon Kang [ID],[3,4] Keehoon Jung [ID],[2,5,6] Doo Hyun Chung [ID],[7,8]
Sang-Jun Ha [ID],[9] Young-Joon Kim [ID],[3,4*] Hye Young Kim [ID] [1,2,6*]

[1]Laboratory of Mucosal Immunology, Department of Biomedical Sciences, Seoul National University College of Medicine, Seoul, Korea
[2]Department of Biomedical Sciences, BK21 Plus Biomedical Science Project, Seoul National University College of Medicine, Seoul, Korea
[3]Genome Research Center, Department of Biochemistry, College of Life Science and Biotechnology, Yonsei University, Seoul, Korea
[4]Department for Integrated OMICS for Biomedical Science, Yonsei University, Seoul, Korea
[5]Department of Anatomy and Cell Biology, Seoul National University College of Medicine, Seoul, Korea
[6]Institute of Allergy and Clinical Immunology, Seoul National University Medical Research Center, Seoul, Korea
[7]Department of Pathology, Seoul National University College of Medicine, Seoul, Korea
[8]Laboratory of Immune Regulation, Department of Biomedical Sciences, Seoul National University College of Medicine, Seoul, Korea
[9]System Immunology Laboratory, Department of Biochemistry, College of Life Science and Biotechnology, Yonsei University, Seoul, Korea

OPEN ACCESS

Correspondence to
Young-Joon Kim, PhD
Genome Research Center, Department of Biochemistry, College of Life Science and Biotechnology, Department for Integrated OMICs for Biomedical Science, Yonsei University, 50, Yonsei-ro, Seodaemun-gu, Seoul 03722, Korea.
Email: yjkim@yonsei.ac.kr

Hye Young Kim, PhD
Laboratory of Mucosal Immunology, Department of Biomedical Sciences, Department of Biomedical Sciences, BK21 Plus Biomedical Science Project, Seoul National University College of Medicine, Institute of Allergy and Clinical Immunology, Seoul National University Medical Research Center, 103, Daehak-ro, Jongno-gu, Seoul 03080, Korea.
Email: hykim11@snu.ac.kr

https://e-aair.org

ABSTRACT

Purpose: Three observations drove this study. First, 2′-5′-oligoadenylate synthetase-like protein (OASL) is a negative regulator of type I interferon (IFN). Second, type I IFN plays a central role during virus infections and the pathogenesis of various diseases, including asthma. Third, influenza A virus (IAV) causes non-eosinophilic asthma. To evaluate the potential relationships between OASL, type I IFN, and pulmonary innate immune cells in IAV-induced acute airway inflammation by using $Oasl1^{-/-}$ mice.

Methods: Asthma was induced in wild-type (WT) and $Oasl1^{-/-}$ mice with IAV or ovalbumin (OVA). Airway hyperreactivity (AHR) and immune cell infiltration in the bronchoalveolar lavage (BAL) fluids were measured. The immune cells in the lungs were analyzed by flow cytometry. To investigate the ability of type I IFN to shape the response of lung type 2 innate lymphoid cells (ILC2s), IFN-α was treated intratracheally. Plasmacytoid dendritic cells (pDCs) sorted from bone marrow and ILC2s sorted from lungs of naïve mice were co-cultured with/without interferon-alpha receptor subunit 1 (IFNAR-1)-blocking antibodies.

Results: In the IAV-induced asthma model, $Oasl1^{-/-}$ mice developed greater AHR and immune cell infiltration in the BAL fluids than WT mice. This was not observed in OVA-induced asthma, a standard model of allergen-induced asthma. The lungs of infected $Oasl1^{-/-}$ mice also had elevated DC numbers and $Ifna$ expression and depressed IAV-induced ILC2 responses, namely, proliferation and type 2 cytokine and amphiregulin production. Intratracheal administration of type I IFN in naïve mice suppressed lung ILC2 production of type 2 cytokines and amphiregulin. Co-culture of ILC2s with pDCs showed that pDCs inhibit the function of ILC2s by secreting type I IFN.

Generated by xmlinkpress

ORCID iDs
Yuna Chang
https://orcid.org/0000-0002-4068-3171
Ji-Seon Kang
https://orcid.org/0000-0003-1830-7329
Keehoon Jung
https://orcid.org/0000-0002-2199-5292
Doo Hyun Chung
https://orcid.org/0000-0002-9948-8485
Sang-Jun Ha
https://orcid.org/0000-0002-1192-6031
Young-Joon Kim
https://orcid.org/0000-0001-5061-587X
Hye Young Kim
https://orcid.org/0000-0001-5978-512X

Conclusions: OASL1 may impede the IAV-induced acute airway inflammation that drives AHR by inhibiting IAV-induced type I IFN production from lung DCs, thereby preserving the functions of lung ILC2s, including their amphiregulin production.

Keywords: Oligoadenylate synthetase-like protein; type I interferon; influenza A virus; type 2 innate lymphoid cells; amphiregulin; airway hyperreactivity; dendritic cell; lung; mice

INTRODUCTION

Influenza A viruses (IAV) occur in local outbreaks and pandemics, particularly during winter. They not only cause significant illness in the general community, but they also raise the mortality rates of susceptible populations. They are RNA viruses that are classified into types according to their hemagglutinin (H) and/or neuraminidase (N) antigens.[1] H1N1, H2N2, and H3N2 are the 3 most pathogenic IAV types in humans[2]: while they typically cause fever, cough, sore throat, and myalgia, they can also lead to more serious problems, including pneumonia, respiratory arrest, and neurological illness.[3-5]

During viral infection, the first line of defense is the innate immune system, which mounts anti-viral responses. In particular, once a host cell is penetrated by a virus, the cell recognizes the virus *via* its pattern-recognition receptors (PRRs). These include Toll-like receptor (TLR) 7, which binds to single-stranded viral RNA, and TLR3 and retinoic acid-inducible gene I (RIG-I), which bind to double-stranded viral RNA.[6] The signals transmitted by these PRRs then cause the infected cells to produce anti-viral cytokines, including type I interferons (IFNs) such as IFN-α.[7]

IFNs exert their pleiotropic effects by inducing a variety of IFN-stimulated genes (ISGs).[8,9] Of particular interest is the ISG family called oligoadenylate synthetase (OAS), which has seven members. Among them, two OAS genes bear an OAS-like domain that has changes in the nucleotidyltransferase active site and thus fails to produce functional OASs. These genes encode the OAS-like proteins called oligoadenylate synthetase-like protein (OASL) and OASL1.[10-12] Despite their lack of OAS activity, the OASLs can also limit RNA viral infections by interacting with the RNA sensor RIG-I and enhancing RIG-I-mediated type I IFN production.[13] Conversely, OASLs can promote DNA virus infections by impeding virus-triggered IFN production.[14] OASL1 also negatively regulates the production of type I IFNs by preventing the translation of interferon regulatory factor (IRF) 7.[15] Thus, depending on the stimulus, OASL can both promote and inhibit type I IFN production, thereby shaping the antiviral properties of the innate immune system.

Innate lymphoid cells (ILCs) are lymphocytes that do not express the antigen receptors on T cells and B cells.[16] There are 3 distinct ILC groups, as determined by the different transcription factors that drive their production and the effector cytokines that they express: group 1 ILCs (ILC1s), group 2 ILCs (ILC2s), and group 3 ILCs (ILC3s).[17] Of these, the ILC2s, which are driven by GATA-3 and produce type 2 cytokines (interleukin [IL]-5 and IL-13), play essential roles in mucosal immunity, particularly in the lung.[18,19] Thus, when the lung is stimulated by viruses or other asthmogenic triggers, these lung-residing cells become rapidly activated by epithelial cell-derived cytokines, namely, IL-33 and IL-25. This induces the ILC2s to produce IL-5 and IL-13, which in turn leads to eosinophil recruitment, mucus secretion, goblet cell hyperplasia, and airway hyperreactivity (AHR).[20,21] Notably, lung ILC2s also secrete

amphiregulin, which promotes airway epithelial cell proliferation and tissue regeneration after virus-induced tissue damage, and helps resolve virus-induced inflammation.[19] Thus, the functions of ILC2s against virus can vary from worsening inflammation (due to their type 2 cytokine production[22]) to generating protective immunity by secreting amphiregulin.[19]

In the present study, we explored the effect of knocking out *Oasl1* on the ability of IAV to induce excessive lung inflammation. We found that during the acute phase of IAV infection, *Oasl1*^{-/-} mice exhibited worse lung inflammation and AHR than wild-type (WT) mice. Thus, OASL1 appears to suppress IAV-induced asthma. Further experiments then showed that compared to IAV-infected WT mice, the infected *Oasl1*^{-/-} mice had increased dendritic cells (DCs) and fewer ILC2s in the lung. Since (i) OASL can shape type I IFN production, (ii) type I IFNs play essential roles in antiviral innate immune host responses, (iii) type I IFN can downregulate ILC2s, and (iv) DCs are key producers of type I IFN in viral infections, we speculated that the effect of *Oasl1* deletion on ILC2s was mediated by DC-produced type I IFN. Indeed, the infected *Oasl1*^{-/-} mice had higher lung levels of *Ifna* genes than infected WT mice. Moreover, intratracheal injections of type I IFN in naïve mice reduced lung ILC2 functions, and co-culture of ILC2s with plasmacytoid dendritic cells (pDCs) inhibited the function of ILC2s by type I IFN. Thus, OASL1 may contribute to lung homeostasis by maintaining the ILC2s population during IAV infection, thereby preserving the function of these innate immune cells and protecting the lung from IAV-induced lung inflammation.

MATERIALS AND METHODS

Mice
C57BL/6 WT mice were obtained from the Koatech Company (Pyeongtaek, Korea). *Oasl1*^{-/-} mice on the C57BL/6 background were derived from our previous study by a standard gene-targeting strategy with embryonic stem cells.[15] Seven-week-old female mice were used for experiments. All mice were maintained in specific pathogen-free facilities on a 12-hour light/12-hour dark cycle and were provided food and water ad libitum. The IAV infection- and ovalbumin (OVA)-induced asthma model animal experiments were approved by the Institutional Animal Care and Use Committee (IACUC) in Yonsei University. The IFN-α treatment experiment was approved by the IACUC in Seoul National University Hospital. The animals were maintained in a facility that was accredited by AAALAC International (#001169) and that follows the Guide for the Care and Use of Laboratory Animals, 8th edition, NRC (2010).

Induction of asthma
To generate the IAV-induced asthma model, mice were anesthetized with 1.5% isoflurane and then infected intranasally with 1.5×10^6 plaque-forming units of IAV (New Caledonia/20/99 H1N1 strain) in 50 μL phosphate-buffered saline (PBS) per mouse or the same volume of PBS. On day 5 after virus infection, mice were sacrificed. For OVA-induced asthma, mice were sensitized with intraperitoneal administrations of 100 μg OVA-2 mg alum on day 0 followed by intranasal challenges with 50 μg OVA on days 14, 21, 22, and 23. Mice were sacrificed on day 24. After sacrifice, the lung and bronchoalveolar lavage (BAL) fluids were collected for analysis.

IFN-α administration
Mice were treated for 3 consecutive days by intratracheal injections of 300 ng IFN-α (BioLegend, San Diego, CA, USA) in 50 μL PBS. The mice were sacrificed 3 days after the last challenge, and the lungs were collected for analysis.

Measurement of AHR

Airway responsiveness was measured in conscious animals by using whole body barometric plethysmography (Buxco, Troy, NY, USA). Increases in enhanced pause (Penh) were used as an index of airway obstruction. Briefly, mice were placed in the main chamber and baseline readings were taken for 3 minutes and then averaged. The mice were then nebulized for 3 minutes with increasing concentrations (10–80 mg/mL) of methacholine (Sigma-Aldrich, St. Louis, MO, USA). After each nebulization, the readings were taken for 3 minutes and averaged. AHR was expressed as fold increases in Penh values for each concentration of methacholine compared with Penh values after PBS challenge.

BAL fluid cytology and lung histology

BAL fluid was collected from the lung by inserting an 18G catheter into the trachea and gently washing the bronchioles 3 times with 1 mL sterile PBS containing 2% fetal bovine serum (FBS). BAL fluid cells were attached to slides by centrifugation using a Shandon™ Cytospin (Thermo Fisher Scientific, Waltham, MA, USA). The cells were stained with DiffQuick (Sysmex, Kobe, Japan) and the infiltrating cells were counted. Lung tissues were fixed with 4% formaldehyde for at least 24 hours, embedded in paraffin, and stained with hematoxylin and eosin (H&E). All bright field microscopy images were captured by using the Olympus IX53 microscope (Olympus, Center Valley, PA, USA) with 20X apochromatic objective lenses and an Olympus color CCD camera.

Single cell isolation from lung tissue

Lung tissues were minced with single-edge blades and digested in 5 mL RPMI medium containing type IV collagenase (1 mg/mL, Worthington, Lakewood, NJ, USA) for 1 hour at 37°C with shaking. After incubation, the cell suspensions were filtered with nylon mesh. The red blood cells were then lysed by Red Blood Cell Lysing Buffer (Sigma-Aldrich). After washing with PBS, the cells were resuspended in an appropriate volume of buffer and subjected to flow cytometry, as described below.

Quantitative polymerase chain reaction

Tissues were homogenized using PowerMasher (Optima, Tokyo, Japan) with Trizol® Reagent (Invitrogen, Carlsbad, CA, USA). After extracting total RNA, cDNA was synthesized using iScript™ cDNA Synthesis Kit (Bio-Rad, Hercules, CA, USA). Quantitative real-time polymerase chain reaction (PCR) was performed using iQ™ SYBR® Green Supermix (Bio-Rad) and PrimeTime® qPCR Assays (Integrated DNA Technologies, Coralville, IA, USA). Gene expression of each target was calculated relative to the house-keeping gene *Gapdh*.

Flow cytometry

Single-cell suspensions from lung tissues were blocked with anti-mouse CD16/CD32 (BD Bioscience, Franklin Lakes, NJ, USA) and stained with the following monoclonal antibodies: Brilliant Violet (BV) 421-anti-Siglec-F (BD Biosciences), Allophycocyanin (APC)-anti-F4/80, anti-CD11b (BioLegend), BV650-anti-CD45 (BioLegend), Fluorescein isothiocyanate (FITC)-anti-F4/80, Lineage cocktail (anti-CD3, anti-CD11b, anti-CD11c, anti-CD19, anti-CD49b, anti-F4/80, anti-FcεRIα) (BioLegend), PE-anti-CD11c, PE/Cy7-anti-CD11c, anti-CD127, anti-Ly-6G, PerCP/Cy5.5-anti-CD45 (BioLegend), and TexasRed-anti-CD45 (Invitrogen). For intracellular cytokine staining of lymphoid cells, single cells were incubated in RPMI medium containing 10% FBS with phorbol 12-myristate 13-acetate (PMA) (100 ng/mL, Sigma-Aldrich), ionomycin (1 µg/mL, Sigma-Aldrich), and BD GolgiStop™ (0.7 µL/mL, BD Bioscience) at 37°C for 4 hours. For intracellular cytokine staining of myeloid cells, single cells were incubated in RPMI medium

containing 10% FBS with lipopolysaccharide (LPS) (10 ng/mL, Merck, Darmstadt, Germany), and BD GolgiStop™ (0.7 μL, BD Bioscience). at 37°C for 2 hours. After surface staining, the cells were fixed and permeabilized with Foxp3/Transcription Factor Fixation/Permeabilization Buffer set (Invitrogen). Finally, the cells were stained with the following monoclonal antibodies: BV421-anti-GATA3 (BD Bioscience), APC-anti-IL-5, anti-T-bet (BioLegend), BV421-anti-IL-17A (BioLegend), FITC-anti-IL-1β (BioLegend), PE-anti-IFN-γ, anti-IL-13, anti-T-bet, anti-TNF-α (BioLegend), and PerCP/Cy5.5-anti-IFN-γ (BioLegend). The cells were analyzed by using a BD LSRII flow cytometer and FACS Diva software (BD Biosciences). Flow cytometry data were analyzed by using Flow Jo analysis software (Treestar, Ashland, OR, USA).

Enzyme-linked immunosorbent assays (ELISA)

The levels of mouse IL-5 and IL-13 were measured by sandwich ELISA. 96 Well EIA/RIA Plates (Corning, NY, USA) and DuoSet® ELISA Development Systems (R&D Systems, Minneapolis, MN, USA) were used according to the manufacturers' instructions. Results were read at an optical density of 450 nm by using a Sunrise™ microplate reader and Magellan V7.2 software (Tecan, Männedorf, Switzerland).

Co-culture of type 2 ILCs and pDCs

ILC2s were isolated from the lungs of naïve mice by using EasySep™ Mouse Pan-ILC Enrichment Kit (STEMCELL Technologies, Vancouver, Canada) according to the manufacturer's instructions. pDCs were isolated from bone marrows of naïve mice using EasySep™ Mouse Plasmacytoid DC Isolation Kit (STEMCELL Technologies, Vancouver, Canada) according to the manufacturer's instructions. Thus, bone marrow was flushed out with PBS and filtered with a 40-μm strainer. Red blood cells were lysed by RBC Lysis Buffer (BioLegend) and the cells were washed with PBS. Sorted 1.0×10^5 ILC2s were cultured with 1.0×10^5 pDCs in DMEM media at 37°C, 5% CO_2. Recombinant IL-2 (10 ng/mL, BioLegend), IL-7 (10 ng/mL, BioLegend), IL-33 (10 ng/mL, BioLegend), and ssRNA40 (1 μg/mL, Invitrogen) were simultaneously added into the co-culture plate. In some groups, anti-mouse interferon-alpha receptor subunit 1 (IFNAR-1) (20 μg/mL, BioXCell, Lebanon, NH, USA) was added in co-culture. After 48 hours, the cells were analyzed by flow cytometry, and the supernatant was analyzed by ELISA.

Statistical analysis

All statistical analyses were performed using GraphPad Prism7 (Graph Pad Software, San Diego, CA, USA). Data normality was based on Shapiro-Wilk test. Two unpaired groups were compared by using two-tailed Student's *t*-test (parametric variables) or Mann-Whitney U test (nonparametric variables). When multiple groups were compared, two-way ANOVA followed by Tukey's multiple comparison test was used. The data are presented as arithmetic means with the standard error of the mean (SEM). $P < 0.05$ was considered statistically significant. Statistical methods to predetermine sample size were not used; rather, sample sizes were based on prior experience with similar studies.

RESULTS

Oasl1 deletion associates with increased pulmonary inflammation and AHR in a model of IAV infection-induced asthma

To elucidate the role of OASL1 in IAV infection, we inoculated WT and *Oasl1*-/- mice intranasally with influenza virus H1N1 (New Caledonia/20/99) and collected the lung tissues
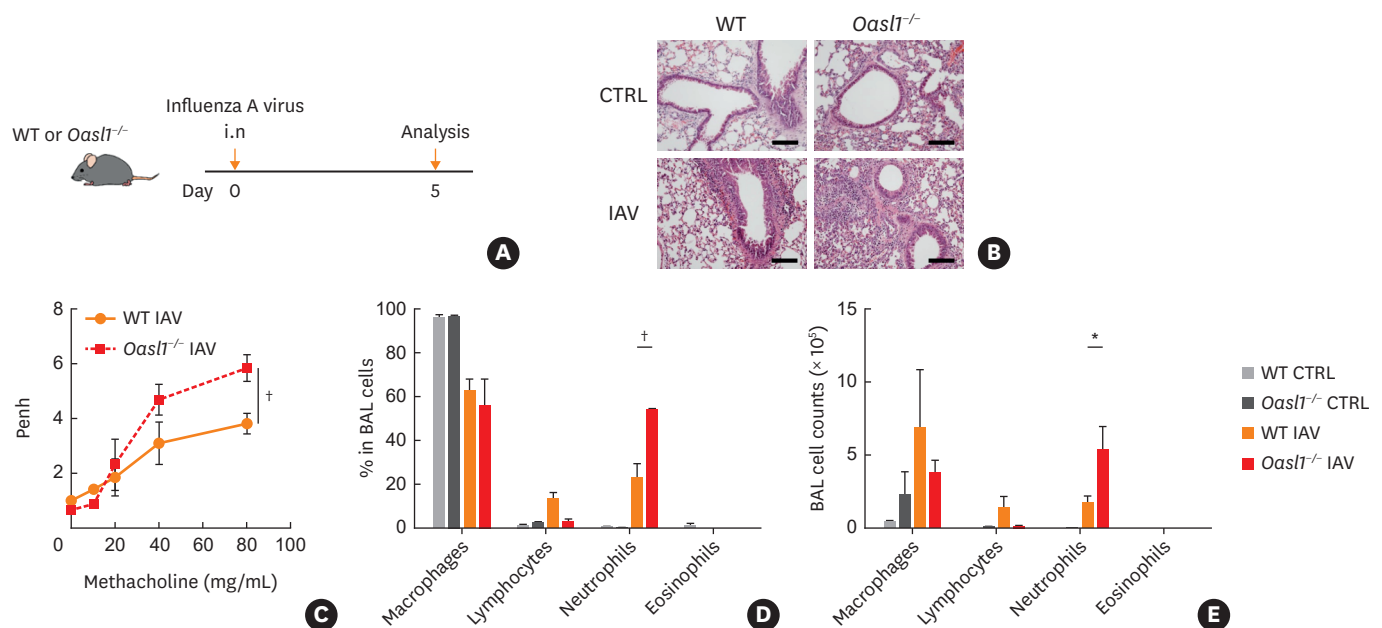
Fig. 1. Influenza A virus infection induces more intensive lung inflammation in *Oasl1*⁻/⁻ mice. (A) Experimental schedule of IAV-induced asthma. (B) Photomicrographs of hematoxylin and eosin stained histological sections of the lungs 5 days after IAV infection (scale bar: μm). (C) Airway hyperreactivity in response to increasing dose of methacholine (0–80 mg/mL) was measured on day 5. Data are presented as mean ± SEM. (D-E) The percentage (D) and absolute number (E) of immune cells in BAL fluids from WT and *Oasl1*⁻/⁻ mice. Data are presented as mean ± SEM (two-way ANOVA). Data representative of three independent experiments with n = 3 per group.
WT, wild-type; IAV, influenza A virus; BAL, bronchoalveolar lavage.
$^*P < 0.05$; $^†P < 0.01$.

and BAL fluids 5 days after infection (**Fig. 1A**). Lung H&E staining showed that compared to the infected WT mice, the infected *Oasl1*⁻/⁻ mice exhibited more severe peribronchiolar and perivascular infiltration of inflammatory cells (**Fig. 1B**). Notably, the infected *Oasl1*⁻/⁻ mice also developed greater AHR (**Fig. 1C**). In addition, analysis of the infiltrating BAL cells showed that the infection increased recruitment of neutrophils into the airways and that the *Oasl1* deletion significantly increased this recruitment (**Fig. 1D and E**). Also, mRNA expression levels of *Tnf*, *Il6*, and *Il10* were increased in the infected *Oasl1*⁻/⁻ mice, although there was no difference in that of *Il8* (**Supplementary Fig. S1**). Thus, *Oasl1* deficiency aggravates lung inflammation during the early phase of IAV infection.

Oas1 deletion does not enhance pulmonary inflammation and AHR in the OVA-induced asthma model

Since *Oasl1* deletion increased IAV-induced AHR, we asked whether this deletion also augmented AHR in another model of asthma, namely, OVA-induced asthma (**Fig. 2A**). WT and *Oasl1*⁻/⁻ mice were sensitized and challenged with OVA, and the resulting lung inflammation and AHR were measured. Unlike in IAV-induced asthma, *Oasl1* deletion had no effect on the extent of immune cell infiltration into the lungs (**Fig. 2B**) or AHR (**Fig. 2C**). Analysis of the inflammatory cells in the BAL fluids showed that the OVA challenge predominantly increased eosinophil numbers in WT mice; however, *Oasl1* deletion had no effect on this pattern (**Fig. 2D and E**). These results together suggest that OASL1 may suppress pulmonary inflammation and AHR by shaping virus-specific inflammatory responses rather than overall pulmonary inflammation.
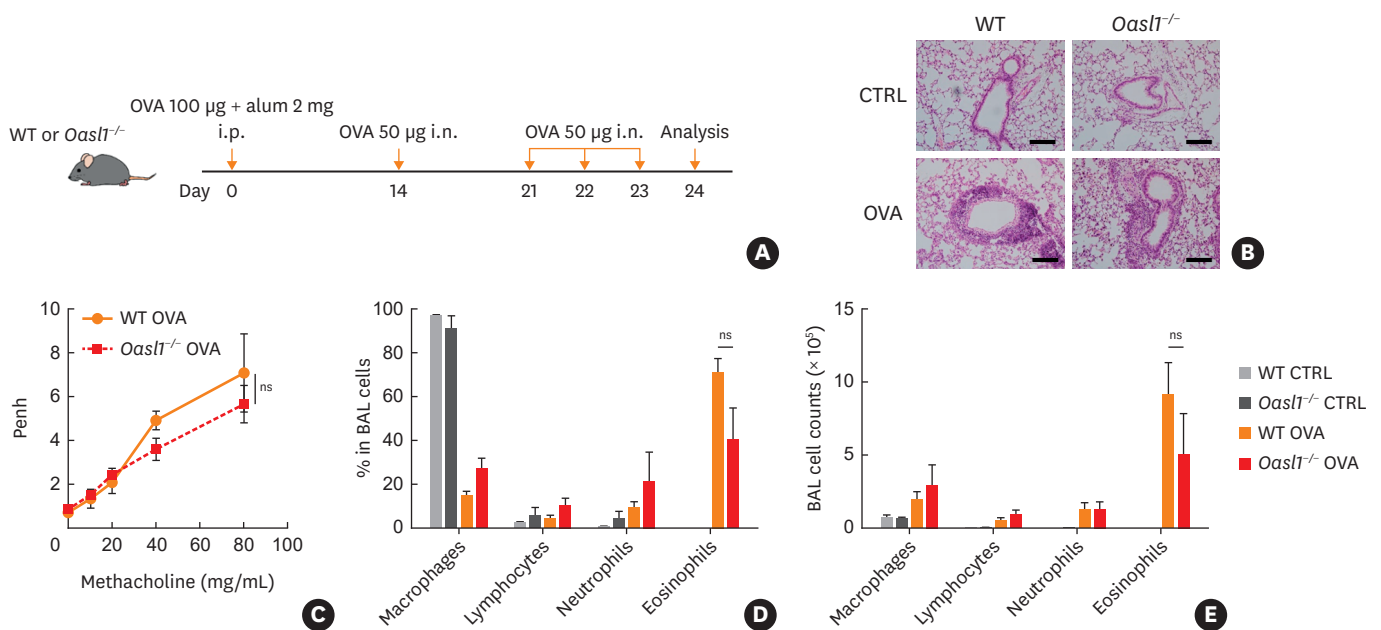
Fig. 2. WT and *Oasl1*⁻/⁻ mice showed no difference in OVA-induced asthma. (A) Experimental schedule of OVA-induced asthma. (B) Photomicrographs of hematoxylin and eosin stained histological sections of lungs from control and asthma induced mice (scale bar: μm). (C) Airway hyperreactivity in response to increasing dose of methacholine (0–80 mg/mL) was measured. Data are presented as mean ± SEM. (D-E) The percentage (D) and absolute number (E) of immune cells in BAL fluids from WT and *Oasl1*⁻/⁻ mice. Data are presented as mean ± SEM (two-way ANOVA). Data representative of three independent experiments with n = 3 per group.
WT, wild-type; OVA, ovalbumin; BAL, bronchoalveolar lavage.
ns, not significant ($P > 0.05$).

Oasl1 deletion further increases the dendritic cell frequencies in IAV-infected lungs

Next, we assessed the inflammatory cell populations in the lungs of the WT and *Oasl1*⁻/⁻ mice after IAV infection more closely (**Supplementary Fig. S2**). Since neutrophils and eosinophils play critical roles in the development of asthma, we initially focused on these cells. We noted that the *Oasl1* deletion had no effect on the baseline numbers of these cells, and that compared to the IAV-infected WT mice, the infected *Oasl1*⁻/⁻ mice had significantly higher neutrophil numbers but lower eosinophil numbers (**Fig. 3A and B**). Thus, OASL1 appears to limit neutrophil recruitment in IAV infection.

Analysis of the alveolar macrophages (AMs) then showed that the *Oasl1* deletion had no effect AM numbers (**Fig. 3C**). The percentage of interstitial macrophages (IM) decreased in *Oasl1*⁻/⁻ mice under normal conditions, but there was no difference in number between WT and *Oasl1*⁻/⁻ mice before and after IAV infection (**Fig. 3D**). With regard to the DCs, the *Oasl1* deletion had no effect on the baseline DC numbers, infection increased them in WT mice, and the *Oasl1* deletion further upregulated this increase (**Fig. 3E**).

Since DCs can counter viral infections by stimulating T cells,[23] we then explored whether the increased DCs in the IAV-infected *Oasl1*⁻/⁻ lungs aggravated pulmonary inflammation by stimulating T cells. Thus, we measured the population and cytokine production of the lung T cells by flow cytometry. However, there was no difference of the percentage of lung T cells of the infected WT and *Oasl1*⁻/⁻ mice and they produced similar amounts of IFN-γ, IL-5, IL-13, and IL-17A (**Fig. 3F and G**). Thus, the elevated DCs in the infected *Oasl1*⁻/⁻ mice were not promoting lung inflammation by activating T cells.
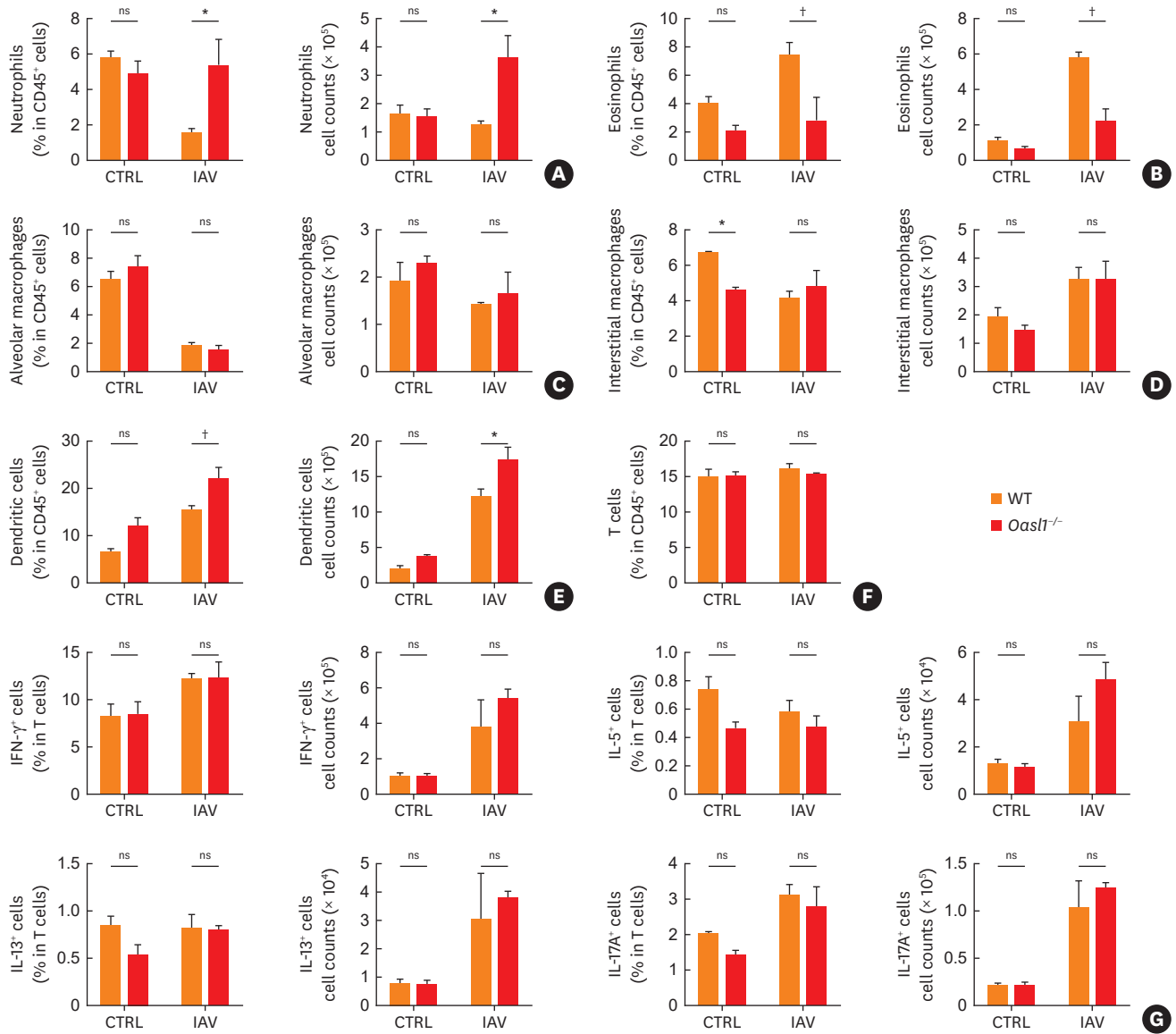
Fig. 3. Changes in pulmonary immune cells in response to IAV infection. 5 days after IAV infection, immune cells in the lungs from WT and *Oasl1*^{−/−} mice were analyzed by flow cytometry. (A-E) The percentage and absolute number of myeloid cells including neutrophils (A, CD45+CD11b+Ly-6G+), eosinophils (B, CD45+CD11b+Siglec-F+), alveolar macrophages (C, CD45+CD11c+F4/80+), and interstitial macrophages (D, CD45+CD11c−F4/80+) and dendritic cells (E, CD45+CD11c+F4/80−) in the lungs of control and IAV-infected mice. Data are presented as mean ± SEM (Two-Way ANOVA). (F) The percentage of total T cells in the lungs of control and IAV-infected WT or *Oasl1*^{−/−} mice. Data are presented as mean ± SEM (Two-Way ANOVA). (G) The percentage and absolute number of IFN-γ+, IL-5+, IL-13+, and IL-17A+ T cells in the lungs of control and IAV-infected WT or *Oasl1*^{−/−} mice. Data are presented as mean ± SEM (two-way ANOVA). Data representative of three independent experiments with n = 3 per group.
IAV, influenza A virus; WT, wild-type; IFN, interferon; IL, interleukin.
*$P < 0.05$; †$P < 0.01$; ns, not significant ($P > 0.05$).

Oasl1 deletion decreases ILC2 numbers and functions after IAV infection

ILCs are the innate counterpart of T cells and also play an essential role in regulating the immune responses and homeostasis of the lungs.[17,24] Since the infected *Oasl1*^{−/−} mice did not exhibit changes in lung T cell activation, and DCs can activate ILCs,[25] we speculated that the upregulated DCs in the infected *Oasl1*^{−/−} mice could aggravate IAV-induced inflammation by affecting the lung ILCs. Thus, we examined the distribution of ILCs in the lungs from infected WT and *Oasl1*^{−/−} mice. The ILCs were identified by focusing on the IL-7R+ cells that
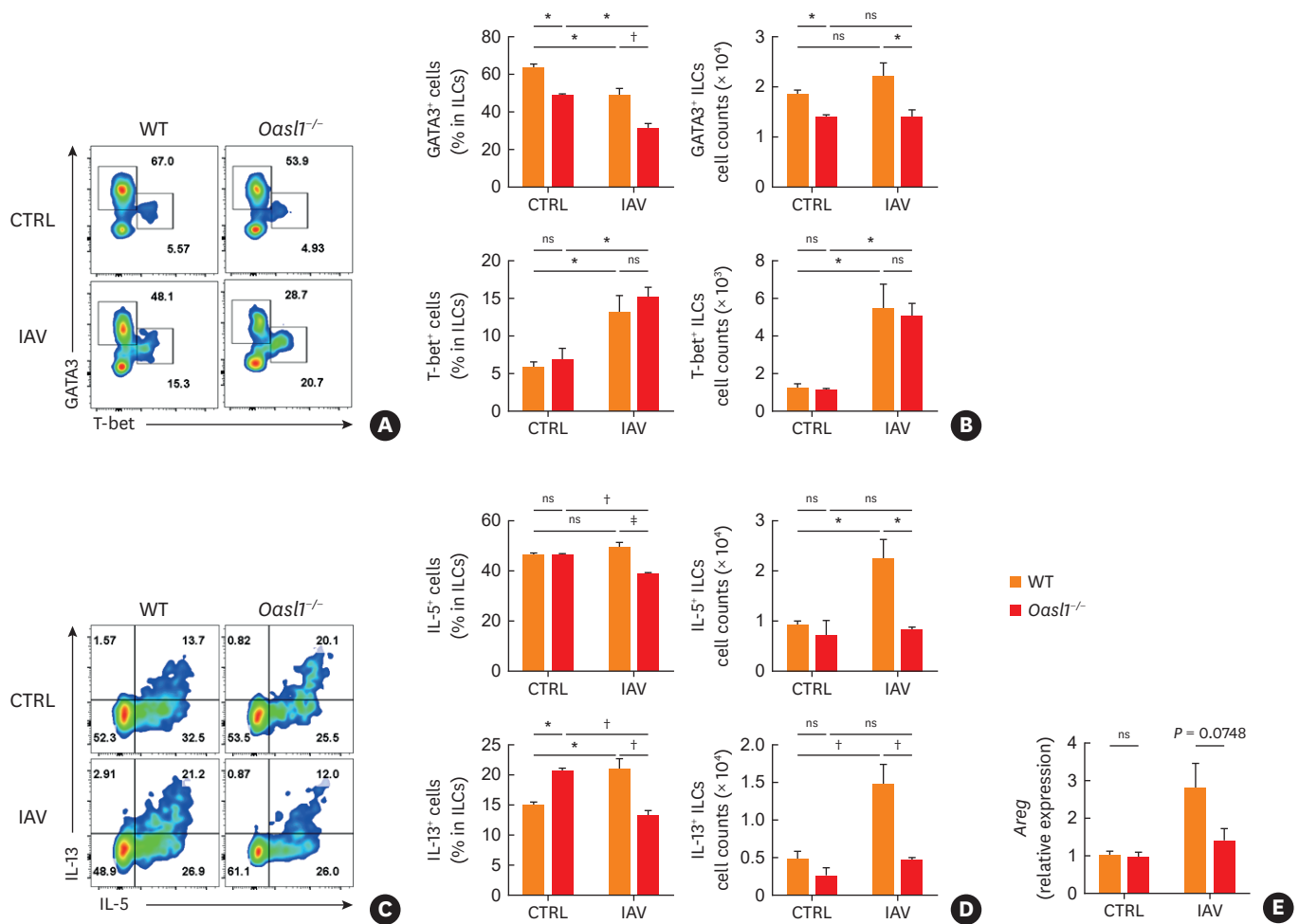
Fig. 4. ILC2s are decreased in naïve and IAV-infected *Oasl1-/-* mice. (A) Representative flow cytometry plots of T-bet+ ILC1s, and GATA3+ ILC2s in the lung of control and IAV-infected mice. (B) The percentage (left) and absolute number (right) of T-bet+ ILC1s, and GATA3+ ILC2s shown in A. Data are presented as mean ± SEM (two-way ANOVA). (C) Representative flow cytometry plots of IL-5+, and IL-13+ ILC2s in the lung of control and IAV-infected mice. (D) The percentage (left) and absolute number (right) of IL-5+, and IL-13+ ILC2s in the lung of control and IAV-infected mice. Data are presented as mean ± SEM (two-way ANOVA). (E) Quantitative PCR analysis of *Areg* in the lung of control and IAV-infected mice. Values are normalized to *Gapdh*. Data are presented as mean ± SEM (two-way ANOVA). Data representative of three independent experiments with n = 3 per group.
IAV, influenza A virus; WT, wild-type; IFN, interferon; IL, interleukin; ILC, innate lymphoid cell; ILC2, type 2 innate lymphoid cell.
*$P < 0.05$; †$P < 0.01$; ‡$P < 0.005$; ns, not significant ($P > 0.05$).

did not express lineage markers (Lin). The ILC subsets were then identified by measuring the subset-specific transcription factors (**Supplementary Fig. S3A**). The *Oasl1* deletion is associated with significantly lower baseline Lin⁻Gata3+ ILC2 frequencies. With IAV infections, the number of Lin⁻Gata3+ ILC2s in *Oasl1-/-* mice was lower than in WT (**Fig. 4A and B**). IAV infection increased the number of Lin⁻T-bet+ ILC1s in both WT and *Oasl1-/-* mice, but there were no differences between groups (**Fig. 4A and B**).

We then looked at the effect of the *Oasl1* deletion on lung ILC2 production of type 2 cytokines after IAV infection. Since ILC2s also secrete amphiregulin in response to IAV,[19] we also examined the mRNA expression of amphiregulin (*Areg*). *Oasl1* deletion generally did not affect the baseline numbers of IL-5 and IL-13-producing ILCs or their *Areg* expression (**Fig. 4C-E**). In line with previous reports,[19,22] IAV infection increased the production of IL-5 and IL-13 by lung ILC2s from WT mice; however, this increase did not occur in the *Oasl1-/-* mice (**Fig. 4C and D**).

Similarly, the infection increased *Areg* expression in WT lung ILCs but not in *Oasl1*^{-/-} lung ILC2s, although this difference did not achieve statistical significance ($P = 0.07$) (**Fig. 4E**). With regard to the IFN-γ-secreting ILC1s, infection elevated their IFN-γ expression to similar levels in the WT and *Oasl1*^{-/-} mice (**Supplementary Fig. S3B and C**). Based on these results, we hypothesized that the *Oasl1* deletion increased the neutrophilic inflammation in the lungs by reducing the numbers of ILC2s and impairing their functions.

Oasl1 deletion increases type I IFN expression and thereby inhibits the numbers and functions of ILC2s

During our explorations to understand how *Oasl1* deletion decreased the numbers and functions of lung ILC2s in IAV infection, we measured the lung levels of the innate cytokines that are known to stimulate ILC2s. However, *Oasl1* deletion did not affect the baseline or IAV-induced levels of *Il33*, *Il25*, and *Tslp* mRNA (**Fig. 5A**). Therefore, we considered other factors that can regulate ILC2s. Recently, it was reported that type I IFN can restrict the function of ILC2s.[26,27] This excited our interest because (i) type I IFN is the potent anti-viral cytokine,[7,8] (ii) compared to WT mice, *Oasl1*-deficient mice have higher serum levels of type I IFNs at baseline and produce much higher type 1 IFN levels in response to viral infection: this is because OASL1 binds to and prevents the translation of IRF7,[15] and (iii) as noted above, the infected *Oasl1*^{-/-} lungs contained increased DC numbers, and we knew that pDCs are an essential cellular source of IFN-α upon various viral infections.[28-30] Thus, we first examined the effect of *Oasl1* deletion on the lung expression of IFNs and ISGs, namely, *Ifna5*, *Ifna13*, *Ifnb1*, *Mx1*, and *Ifng*. As reported previously,[15] *Oasl1*^{-/-} mouse lungs tended to have higher baseline expression of IFNs and ISGs than WT mouse lungs. Infection in WT mice had little effect on *Ifna5*, *Ifna13*, and *Mx1*, but in the *Oasl1*^{-/-} mice, the infection hugely augmented the already upregulated *Ifna5* and *Mx1* levels while sharply decreasing the *Ifna13* levels. With regard to *Ifnb1* and *Ifng* expression, the infection elevated these levels in WT mice, and the *Oasl1* deletion further increased this response (**Fig. 5B**). Moreover, the *Oasl1*^{-/-} ILC2s had marked increases in their IFNAR-1 expression after IAV infection (**Fig. 5C**). Therefore, it is possible that the increased type I IFN expression in the lungs of IAV-infected *Oasl1*^{-/-} mice was responsible for the reduced numbers and functions of their lung ILC2s.

To determine whether elevating the type I IFN levels in the lung can affect lung ILCs, we treated naïve WT mice with intratracheal IFN-α and measured the cytokine production from the lung ILCs (**Fig. 5D**). Indeed, this *in vivo* IFN-α treatment significantly reduced the lung GATA3^{+} ILC2s but not the T-bet[+] ILC1s (**Fig. 5E**, **Supplementary Fig. S4A and B**). The treatment also suppressed the production of IL-5, IL-13, and amphiregulin by the lung ILC2s (**Fig. 5F and G**) while not affecting the lung ILC production of IFN-γ and IL-17A (**Supplementary Fig. S4C and D**). These findings together suggest that the increased lung inflammation in IAV-infected *Oasl1*^{-/-} mice may due to high local type I IFN levels that in turn impaired ILC2s. Thus, OASL1 may suppress IAV-induced lung inflammation by inhibiting local type I IFN production, thereby creating an environment in which ILC2s remain able to respond to the infection.

Plasmacytoid DCs suppress ILC2s by secreting IFN-α

Since pDCs are an essential source of IFN-α upon various viral infections[28-30] and *Oasl1* deletion associated with not only higher IFN-α levels but also greater DC frequencies after IAV infection (**Figs. 3E** and **5B**), we asked whether IFN-α secreted by pDCs can regulate ILC2 functions and numbers. Thus, we isolated ILC2s and pDCs from the lung and bone marrow of naïve mice, respectively, and co-cultured these cells with ssRNA40, which activates mouse TLR7 (**Fig. 6A**). Indeed, the co-culture significantly downregulated ILC2 production of type
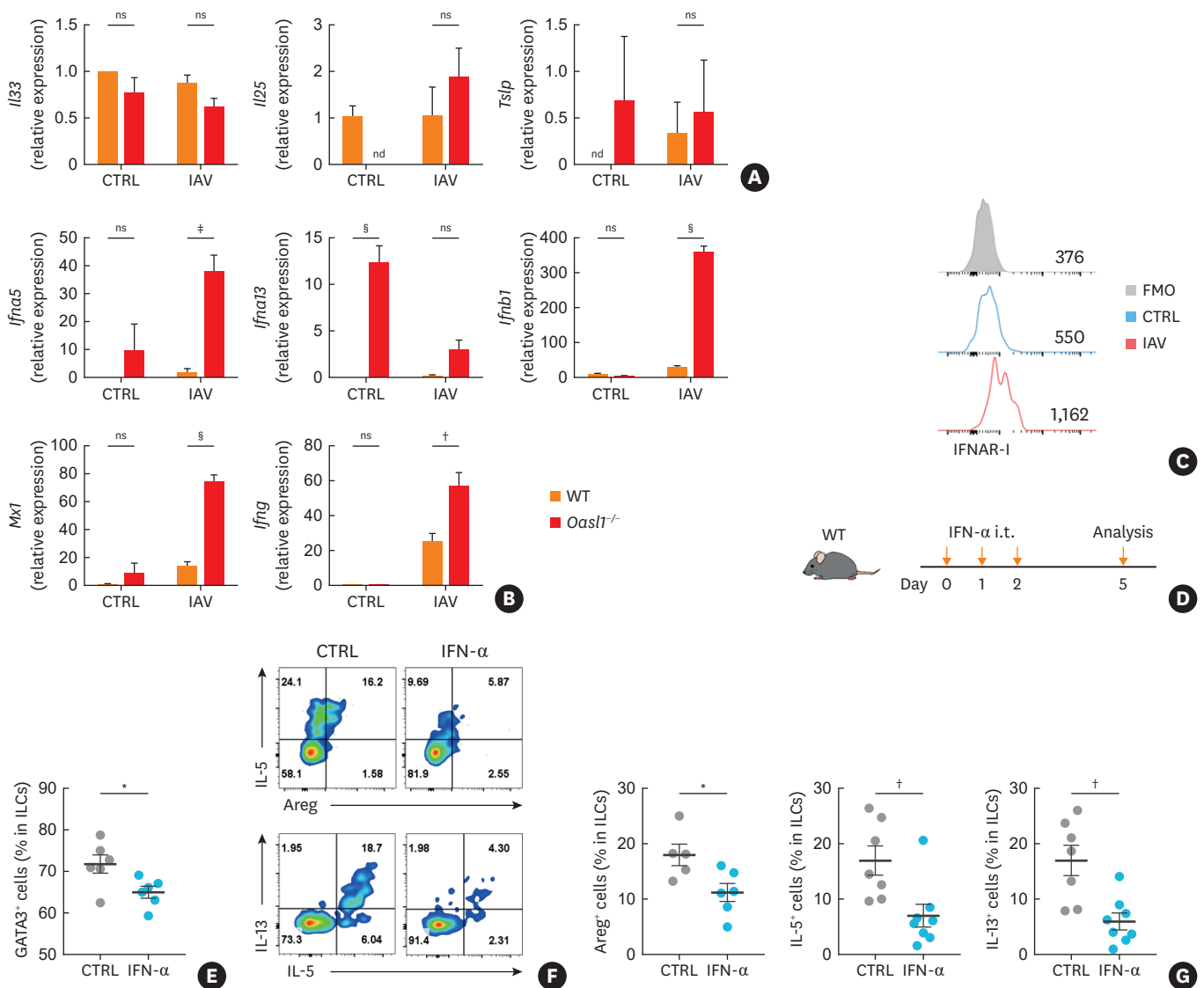
Fig. 5. IAV infection induced Type I IFN, and inhibits ILC2s. (A) Quantitative PCR analysis of *Il33*, *Il25*, and *Tslp* mRNA expression in the lung of control and IAV-infected mice. (B) Quantitative PCR analysis of *Ifna5*, *Infa13*, *Ifnb1*, *Mx1*, and *Ifng* mRNA expression in the lung of control and IAV-infected mice. Values are normalized to *Gapdh*. Data are presented as mean ± SEM (two-way ANOVA). (C) The expression of IFNAR-1 on ILC2s was analyzed by flow cytometry. Histograms show FMO (gray), control (blue), and IAV-infected mice (red). Mean fluorescence intensity is shown on the right side of the histogram. (D) Experimental schedule of IFN-α treatment. (E) The percentage of GATA3+ ILC2s. Data are presented as mean ± SEM (Student's *t*-test). (F) Representative flow cytometry plots of Areg+, IL-5+, and IL-13+ ILC2s in the lung of control and IFN-α treated mice. (G) The percentage of Areg+, IL-5+, and IL-13+ ILC2s. Data are presented as mean ± SEM (Student's *t*-test). Data representative of two independent experiments.
WT, wild-type; IAV, influenza A virus; IFNAR-1, interferon-alpha receptor subunit 1; IFN, interferon; IL, interleukin; ILC, innate lymphoid cell; ILC2, type 2 innate lymphoid cell; PCR, polymerase chain reaction.
*$P < 0.05$; †$P < 0.01$; ‡$P < 0.005$; §$P < 0.001$; ns, not significant ($P > 0.05$).

2 cytokines (IL-5 and IL-13) and amphiregulin (**Fig. 6B and C**, **Supplementary Fig. S5**) and ILC2 proliferation (**Fig. 6D and E**). To confirm that the decreased function of the ILC2s was mediated by IFN-α from pDCs, we added anti-IFNAR antibodies. This blockade of IFN-α signaling caused the cytokine and amphiregulin production and proliferation of the ILC2s to recover strongly despite the presence of the pDCs. Thus, OASL1 may suppress IAV-induced lung inflammation by inhibiting the local type I IFN production of DCs and thereby preserving the function of ILC2s (**Fig. 7**).
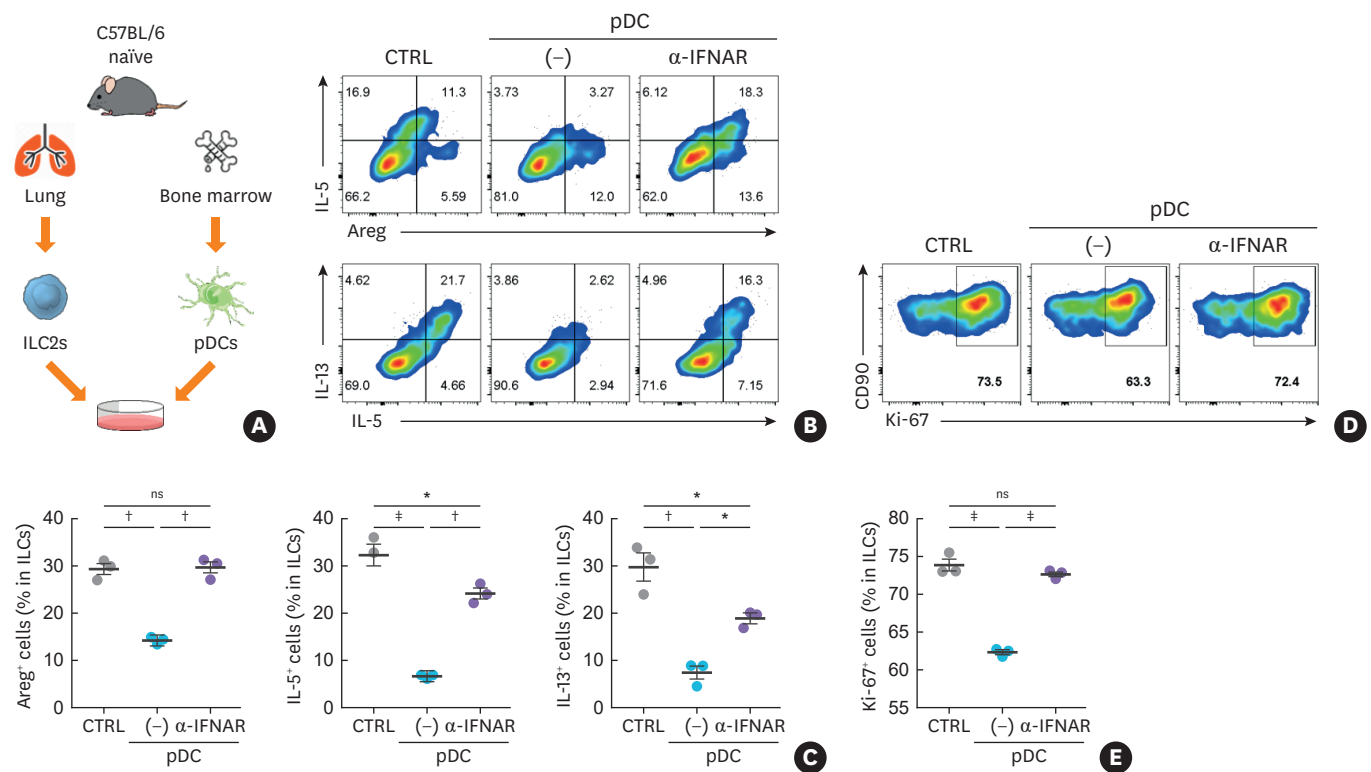
Fig. 6. pDCs suppress ILC2s through secretion of type I IFN. (A) Schematic diagram of co-culture expriment. ILC2s and pDCs were co-cultured with or without anti-IFNAR-1 antibodies for 48 hours. (B-C) The representative flow cytometry plots (B) and the percentage (C) of IL-5^{+}, IL-13^{+}, and Areg[+] ILC2s. Data are presented as mean ± SEM (one-way ANOVA). (D-E) The representative flow cytometry plots (D) and the percentage (E) of Ki-67^{+} ILC2s. Data are presented as mean ± SEM (one-way ANOVA). Data representative of two independent experiments.
pDC, plasmacytoid dendritic cell; ILC2, type 2 innate lymphoid cell; IFNAR, interferon-alpha receptor; IL, interleukin; ILC, innate lymphoid cell.
[*]$P < 0.05$, [†]$P < 0.005$, [‡]$P < 0.001$, ns, not significant ($P > 0.05$).

DISCUSSION

Viral infections, including IAV, are a well-known cause of asthma exacerbations. The present study showed with *Oasl1*-deficient mice that OASL1 protects mice from IAV-induced acute airway inflammation but not from OVA-induced asthma. This effect appears to be mediated by OASL1 inhibition of local type I IFN by DCs, which preserves the functions of lung ILC2s to produce amphiregulin.

Host immunity against viral infection is mediated primarily by type I IFN, which exerts multiple effects by inducing various ISGs.[8,9,31] These ISGs include OASL, which is rapidly induced by virus infection[32] and has been shown to exert anti-viral activities against RNA viruses such as picornavirus[33] by enhancing RIG-I-mediated type I IFN production.[13] However, OASL has also been shown to promote viral persistence.[28,34] Lee *et al.*[28] showed that when *Oasl1*^{-/-} mice were infected with lymphocytic choriomeningitis virus, the elimination of the virus was accelerated. This was associated with high serum type I IFN levels, which were generated by splenic pDCs, and an increased anti-viral CD8^{+} T cell response that was dependent on type I IFN signaling. Similarly, Oh *et al.*[34] showed that when *Oasl1*^{-/-} mice were infected with herpes simplex virus type 2, they exhibited better survival rates and higher type I IFN and cytotoxic T cell responses than WT mice. These studies suggest that OASL1 can suppress type I IFN production during viral infection, thereby promoting viral persistence. By
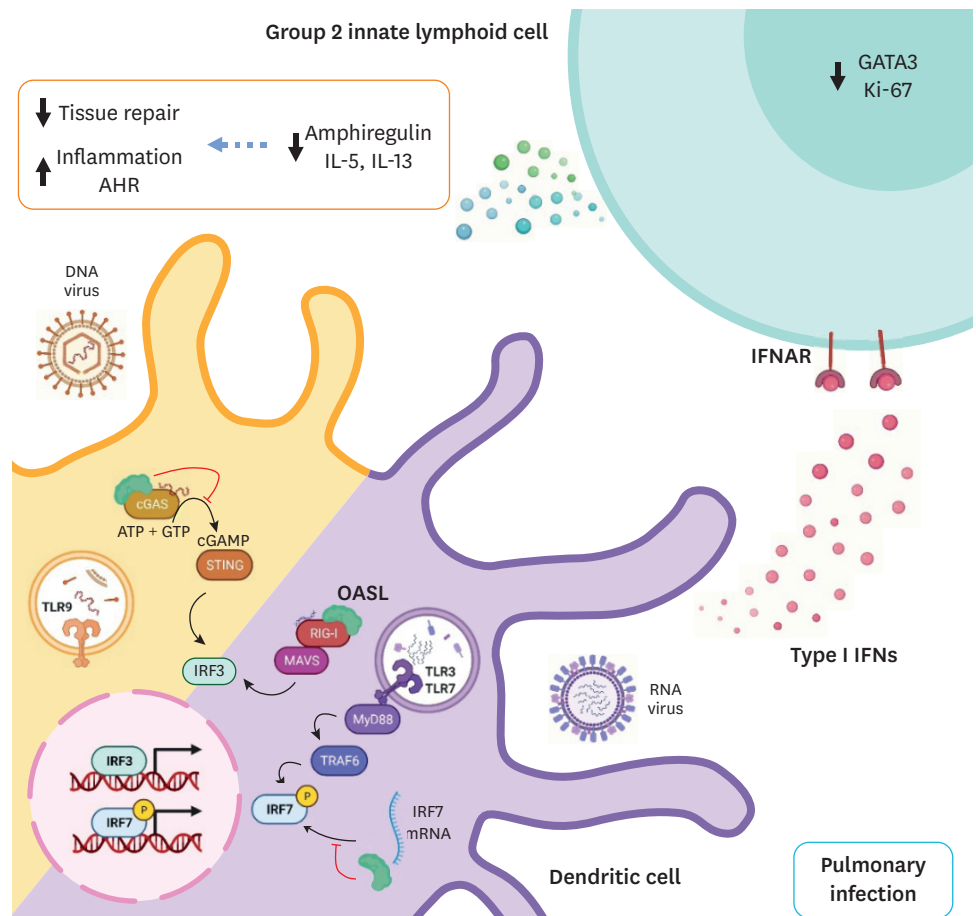
Fig. 7. A schematic figure of the action of OASL in pulmonary viral infection.
Upon DNA viral infection, OASL inhibits type I IFN induction via the cGAS-STING pathway by binding to cGAS and inhibiting cGAS enzymatic activity. During the RNA virus infection, human OASL promotes the type I IFNs by binding to RIG-I and enhancing the sensitivity of RIG-I signaling. On the other hand, mouse OASL1 negatively regulates type I IFN production by binding to IRF7 mRNA and repressing the translation of IRF7. *Oasl1* deficient DCs produce potent amounts of type I IFN in response to IAV infection. Increased type I IFN limits the proliferation and activation of ILC2s. Especially reduced amphiregulin production from ILC2s impairs tissue repair but increases lung inflammation.
AHR, airway hyperreactivity; IL, interleukin; IFNAR, interferon-alpha receptor; TLR, Toll-like receptor; IRF, interferon regulatory factor; OASL, oligoadenylate synthetase-like protein.

contrast, our study shows for the first time that OASL-mediated suppression of type I IFN can also have antiviral effects, in this case on IAV, a pulmonary virus.

Notably, type I and III IFNs are thought to regulate immune responses that play a critical role in asthma pathogenesis,[35,36] although the underlying mechanisms have been explored less than the mechanisms by which IFNs participate in viral infections. Bullens *et al.*[37] reported that the sputum of school-aged asthmatics had higher levels of both IFNλ1 and IFNλ2. Similarly, da Silva *et al.*[36] showed that the sputum of asthmatics with neutrophilic inflammation had elevated levels of type I and III IFN. Finally, Hastie *et al.*[38] showed that sputum IFN-α levels correlated positively with sputum lymphocytes in patients with asthma. Together, these studies suggest that IFN participates in the pathogenesis of asthma.

Our study also showed that OASL1 preserves the function of ILCs by inhibiting IAV-induced type I IFN responses in the lung. This mechanism is supported by recent studies

showing that type I IFN restricts the effector functions of ILC2s, thereby downregulating type 2 inflammation.[26,27] Moreover, ILC2s play essential roles in airway hyperreactivity and inflammation by producing type 2 effector cytokines in an antigen-independent manner.[39,40] However, it should be noted that the roles of ILC2s in the development of virus-induced asthma are more complicated than their roles in other experimental models of asthma: thus, while IL-13-producing ILC2s drive the development of AHR in a murine model of influenza (H3N1) infection,[22] ILC2s also enhance tissue repair after IAV induces acute lung injuries.[19] This complexity is also demonstrated in the present study. Thus, we showed that while IAV infection reduced the number of lung ILC2s, it nevertheless increased the type 2 cytokine production in the ILC2s, which could explain why IAV induced AHR. However, *Oasl1* deficiency led to worse AHR by IAV infection even though the decrease of type 2 cytokines from the ILC2s. What could be the cause of the exacerbated AHR in these mice? We speculate that it reflects the decreased ILC2 production of amphiregulin, which is a growth factor for airway epithelial cells that is known to resolve IAV-induced inflammation in the lung. These findings together suggest that type I IFN responses could influence asthma, especially virus-induced asthma, regardless of the degree of type 2 immune activation. However, further studies are needed to verify this.

The transcription factor IRF7 plays a central role in the regulation of type I IFN production,[41] and He *et al.*[42] recently reported that IRF7 signaling may promote allergic asthma by upregulating ILC2s. Thus, they showed that: papain or IL-33 stimulation dramatically induced IRF7 expression in murine lung ILC2s; IRF7 deficiency impaired the expansion and function of lung ILC2s in several allergic asthma models and induced remission from asthma; and the ILC2s from asthma patients had higher levels of IRF7 than ILC2s from healthy donors.[42] However, in the present study, hampering type I IFN responses by deleting *Oasl1* did not augment the pulmonary inflammation and AHR in the classic OVA-induced allergic asthma model. This difference may reflect the fact that OVA is not a potent stimulant of ILC2s, unlike IL-33 or papain. Moreover, Marichal *et al.*[43] showed that *Irf7* deletion does not affect house dust mite-induced airway inflammation. Interestingly, He *et al.*[42] also found that *Irf7*^{-/-} mice had lower levels of amphiregulin expression on IAV infection than control mice (data not shown), which is consistent with what we found in the *Oasl1*^{-/-} mice. These observations together reflect the complexity of airway inflammation in asthma, which involves several mediators or pathways that influence the lung environment. For example, type I IFN not only has roles in both innate and adaptive immunity, but it is also targeted by other inflammatory mediators; this means that IFNs are likely to play complex roles in respiratory diseases. Thus, when developing asthma treatment strategies, it is essential to understand the mechanisms by which viruses and type I IFN shape asthma.

In conclusion, we showed here that OASL1 suppresses IAV-induced airway inflammation and AHR by inhibiting the virus-induced type I IFN expression of DCs, thereby allowing ILC2s to conduct their activities, including their production of inflammation-resolving amphiregulin. Together, these results demonstrate that OASL1 may be a novel target candidate for the virus-induced exacerbations in asthma.

ACKNOWLEDGMENTS

the experiments. K.J, D.H.C, S.J.H, Y.J.K contributed to the interpretation of the results. Y.C, and H.Y.K. wrote the manuscript. Y.J.K and H.Y.K. supervised the project. The authors declare that they have no competing interests.

SUPPLEMENTARY MATERIALS

Supplementary Fig. S1
The expression of *Tnf*, *Il6*, *Il8*, and *Il10* in the lung of control and IAV-infected WT of Oasl1$^{-/-}$ mice. Quantitative PCR analysis of *Tnf*, *Il6*, *Il8*, and *Il10* mRNA expression in the lung of control and IAV-infected mice. Values are normalized to *Gapdh*. Data are presented as mean ± SEM (two-way ANOVA).

Click here to view

Supplementary Fig. S2
Population of myeloid cells in the lung of control and IAV infected WT or *Oasl1$^{-/-}$* mice. Representative flow cytometry plots of myeloid cells including neutrophils (CD45$^+$CD11b$^+$Ly-6G$^+$) and eosinophils (CD45$^+$CD11b$^+$Siglec-F$^+$), dendritic cells (CD45$^+$CD11c$^+$F4/80$^-$), alveolar macrophages (CD45$^+$CD11c$^+$F4/80$^+$), and interstitial macrophages (CD45+CD11c$^-$F4/80+) in the lung of control and IAV-infected mice.

Click here to view

Supplementary Fig. S3
The expression of IFN-γ and IL-17A of ILCs in the lung of control and IAV-infected WT or *Oasl1$^{-/-}$* mice. (A) Gating strategy of ILC1s (CD45$^+$ Lin-IL-7Rα$^+$ T-bet$^+$) and ILC2s (CD45$^+$ Lin$^-$ IL-7Rα$^+$ GATA3$^+$). (B) Representative flow cytometry plots of IFN-γ$^+$ ILCs in the lung of control and IAV-infected mice. (C) The percentage and absolute number of IFN-γ$^+$ ILCs in the lung of control and IAV-infected mice. Data are presented as mean ± SEM (two-way ANOVA). Data representative of three independent experiments with n = 3 per group.

Click here to view

Supplementary Fig. S4
The expression of IFN-γ and IL-17A of ILCs are not affected by type I IFN. (A) Representative flow cytometry plots of ILC1s and ILC2s in the lung of control and IFN-α-treated mice. (B) The percentage of ILC1s (CD45$^+$Lin$^-$CD127$^+$T-bet$^+$) in the lung of control and IFN-α-treated mice. Data are presented as mean ± SEM (Student's *t*-test). (C) Representative flow cytometry plots of IFN-γ$^+$ and IL-17A$^+$ ILCs in the lung of control and IFN-α-treated mice. (D) The percentage of IFN-γ$^+$ and IL-17A$^+$ ILCs in the lung of control and IFN-α-treated mice. Data are presented as mean ± SEM (Student's *t*-test).

Click here to view

Supplementary Fig. S5
Levels of IL-5 and IL-13 in co-culture experiment of ILC2s with pDCs. ILC2s and pDCs were co-cultured with or without anti-IFNAR-1 antibodies for 48 hours. Levels of IL-5 and IL-13 in the culture supernatant were determined by enzyme-linked immunosorbent assays. Data

Allergy, Asthma &
Immunology Research

AAIR

are presented as mean ± SEM (one-way ANOVA). Data representative of two independent experiments.

Click here to view

REFERENCES

1. Bouvier NM, Palese P. The biology of influenza viruses. Vaccine 2008;26 Suppl 4:D49-53.
   PUBMED | CROSSREF

2. Scholtissek C, Rohde W, Von Hoyningen V, Rott R. On the origin of the human influenza virus subtypes H2N2 and H3N2. Virology 1978;87:13-20.
   PUBMED | CROSSREF

3. Nicholson KG. Clinical features of influenza. Semin Respir Infect 1992;7:26-37.
   PUBMED

4. Cox NJ, Subbarao K. Influenza. Lancet 1999;354:1277-82.
   PUBMED | CROSSREF

5. Paules C, Subbarao K. Influenza. Lancet 2017;390:697-708.
   PUBMED | CROSSREF

6. Mogensen TH. Pathogen recognition and inflammatory signaling in innate immune defenses. Clin Microbiol Rev 2009;22:240-73.
   PUBMED | CROSSREF

7. Bonjardim CA, Ferreira PC, Kroon EG. Interferons: signaling, antiviral and viral evasion. Immunol Lett 2009;122:1-11.
   PUBMED | CROSSREF

8. Sadler AJ, Williams BR. Interferon-inducible antiviral effectors. Nat Rev Immunol 2008;8:559-68.
   PUBMED | CROSSREF

9. Yan N, Chen ZJ. Intrinsic antiviral immunity. Nat Immunol 2012;13:214-22.
   PUBMED | CROSSREF

10. Kristiansen H, Gad HH, Eskildsen-Larsen S, Despres P, Hartmann R. The oligoadenylate synthetase family: an ancient protein family with multiple antiviral activities. J Interferon Cytokine Res 2011;31:41-7.
    PUBMED | CROSSREF

11. Kakuta S, Shibata S, Iwakura Y. Genomic structure of the mouse 2′,5′-oligoadenylate synthetase gene family. J Interferon Cytokine Res 2002;22:981-93.
    PUBMED | CROSSREF

12. Zhu J, Ghosh A, Sarkar SN. OASL-a new player in controlling antiviral innate immunity. Curr Opin Virol 2015;12:15-9.
    PUBMED | CROSSREF

13. Zhu J, Zhang Y, Ghosh A, Cuevas RA, Forero A, Dhar J, et al. Antiviral activity of human OASL protein is mediated by enhancing signaling of the RIG-I RNA sensor. Immunity 2014;40:936-48.
    PUBMED | CROSSREF

14. Ghosh A, Shao L, Sampath P, Zhao B, Patel NV, Zhu J, et al. Oligoadenylate-synthetase-family protein OASL inhibits activity of the DNA sensor cGAS during DNA virus infection to limit interferon production. Immunity 2019;50:51-63.e5.
    PUBMED | CROSSREF

15. Lee MS, Kim B, Oh GT, Kim YJ. OASL1 inhibits translation of the type I interferon-regulating transcription factor IRF7. Nat Immunol 2013;14:346-55.
    PUBMED | CROSSREF

16. Vivier E, Artis D, Colonna M, Diefenbach A, Di Santo JP, Eberl G, et al. Innate lymphoid cells: 10 years on. Cell 2018;174:1054-66.
    PUBMED | CROSSREF

17. Artis D, Spits H. The biology of innate lymphoid cells. Nature 2015;517:293-301.
    PUBMED | CROSSREF

18. Kim HY, Umetsu DT, Dekruyff RH. Innate lymphoid cells in asthma: will they take your breath away? Eur J Immunol 2016;46:795-806.
    PUBMED | CROSSREF

19. Monticelli LA, Sonnenberg GF, Abt MC, Alenghat T, Ziegler CG, Doering TA, et al. Innate lymphoid cells promote lung-tissue homeostasis after infection with influenza virus. Nat Immunol 2011;12:1045-54.
   PUBMED | **CROSSREF**

20. Saenz SA, Siracusa MC, Perrigoue JG, Spencer SP, Urban JF Jr, Tocker JE, et al. IL25 elicits a multipotent progenitor cell population that promotes T(H)2 cytokine responses. Nature 2010;464:1362-6.
   PUBMED | **CROSSREF**

21. Kim HY, Chang YJ, Subramanian S, Lee HH, Albacker LA, Matangkasombut P, et al. Innate lymphoid cells responding to IL-33 mediate airway hyperreactivity independently of adaptive immunity. J Allergy Clin Immunol 2012;129:216-227.e1.
   PUBMED | **CROSSREF**

22. Chang YJ, Kim HY, Albacker LA, Baumgarth N, McKenzie AN, Smith DE, et al. Innate lymphoid cells mediate influenza-induced airway hyper-reactivity independently of adaptive immunity. Nat Immunol 2011;12:631-8.
   PUBMED | **CROSSREF**

23. Lambrecht BN, Hammad H. Lung dendritic cells in respiratory viral infection and asthma: from protection to immunopathology. Annu Rev Immunol 2012;30:243-70.
   PUBMED | **CROSSREF**

24. Barlow JL, McKenzie AN. Innate lymphoid cells of the lung. Annu Rev Physiol 2019;81:429-52.
   PUBMED | **CROSSREF**

25. Briseño CG, Murphy TL, Murphy KM. Complementary diversification of dendritic cells and innate lymphoid cells. Curr Opin Immunol 2014;29:69-78.
   PUBMED | **CROSSREF**

26. Duerr CU, McCarthy CD, Mindt BC, Rubio M, Meli AP, Pothlichet J, et al. Type I interferon restricts type 2 immunopathology through the regulation of group 2 innate lymphoid cells. Nat Immunol 2016;17:65-75.
   PUBMED | **CROSSREF**

27. Moro K, Kabata H, Tanabe M, Koga S, Takeno N, Mochizuki M, et al. Interferon and IL-27 antagonize the function of group 2 innate lymphoid cells and type 2 innate immune responses. Nat Immunol 2016;17:76-86.
   PUBMED | **CROSSREF**

28. Lee MS, Park CH, Jeong YH, Kim YJ, Ha SJ. Negative regulation of type I IFN expression by OASL1 permits chronic viral infection and CD8^{+} T-cell exhaustion. PLoS Pathog 2013;9:e1003478.
   PUBMED | **CROSSREF**

29. Fitzgerald-Bocarsly P, Dai J, Singh S. Plasmacytoid dendritic cells and type I IFN: 50 years of convergent history. Cytokine Growth Factor Rev 2008;19:3-19.
   PUBMED | **CROSSREF**

30. Wolf AI, Buehler D, Hensley SE, Cavanagh LL, Wherry EJ, Kastner P, et al. Plasmacytoid dendritic cells are dispensable during primary influenza virus infection. J Immunol 2009;182:871-9.
   PUBMED | **CROSSREF**

31. Sen GC, Sarkar SN. The Interferon-stimulated genes: targets of direct signaling by interferons, double-stranded RNA, and viruses. In: Pitha PM, editor. Interferon: The 50th Anniversary. Berlin, Heidelberg: Springer Berlin Heidelberg; 2007. 233-50.

32. Melchjorsen J, Kristiansen H, Christiansen R, Rintahaka J, Matikainen S, Paludan SR, et al. Differential regulation of the OASL and OAS1 genes in response to viral infections. J Interferon Cytokine Res 2009;29:199-208.
   PUBMED | **CROSSREF**

33. Marques J, Anwar J, Eskildsen-Larsen S, Rebouillat D, Paludan SR, Sen G, et al. The p59 oligoadenylate synthetase-like protein possesses antiviral activity that requires the C-terminal ubiquitin-like domain. J Gen Virol 2008;89:2767-72.
   PUBMED | **CROSSREF**

34. Oh JE, Lee MS, Kim YJ, Lee HK. OASL1 deficiency promotes antiviral protection against genital herpes simplex virus type 2 infection by enhancing type I interferon production. Sci Rep 2016;6:19089.
   PUBMED | **CROSSREF**

35. Kalinowski A, Galen BT, Ueki IF, Sun Y, Mulenos A, Osafo-Addo A, et al. Respiratory syncytial virus activates epidermal growth factor receptor to suppress interferon regulatory factor 1-dependent interferon-lambda and antiviral defense in airway epithelium. Mucosal Immunol 2018;11:958-67.
   PUBMED | **CROSSREF**

36. da Silva J, Hilzendeger C, Moermans C, Schleich F, Henket M, Kebadze T, et al. Raised interferon-β, type 3 interferon and interferon-stimulated genes - evidence of innate immune activation in neutrophilic asthma. Clin Exp Allergy 2017;47:313-23.
   PUBMED | **CROSSREF**

37. Bullens DM, Decraene A, Dilissen E, Meyts I, De Boeck K, Dupont LJ, et al. Type III IFN-λ mRNA expression in sputum of adult and school-aged asthmatics. Clin Exp Allergy 2008;38:1459-67.
    PUBMED | CROSSREF

38. Hastie AT, Steele C, Dunaway CW, Moore WC, Rector BM, Ampleford E, et al. Complex association patterns for inflammatory mediators in induced sputum from subjects with asthma. Clin Exp Allergy 2018;48:787-97.
    PUBMED | CROSSREF

39. Halim TY, MacLaren A, Romanish MT, Gold MJ, McNagny KM, Takei F. Retinoic-acid-receptor-related orphan nuclear receptor alpha is required for natural helper cell development and allergic inflammation. Immunity 2012;37:463-74.
    PUBMED | CROSSREF

40. Barlow JL, Bellosi A, Hardman CS, Drynan LF, Wong SH, Cruickshank JP, et al. Innate IL-13-producing nuocytes arise during allergic lung inflammation and contribute to airways hyperreactivity. J Allergy Clin Immunol 2012;129:191-198.e4.
    PUBMED | CROSSREF

41. Honda K, Yanai H, Negishi H, Asagiri M, Sato M, Mizutani T, et al. IRF-7 is the master regulator of type-I interferon-dependent immune responses. Nature 2005;434:772-7.
    PUBMED | CROSSREF

42. He J, Yang Q, Xiao Q, Lei A, Li X, Zhou P, et al. IRF-7 is a critical regulator of type 2 innate lymphoid cells in allergic airway inflammation. Cell Reports 2019;29:2718-2730.e2716.
    PUBMED | CROSSREF

43. Marichal T, Bedoret D, Mesnil C, Pichavant M, Goriely S, Trottein F, et al. Interferon response factor 3 is essential for house dust mite-induced airway allergy. J Allergy Clin Immunol 2010;126:836-844.e813.
    PUBMED | CROSSREF